Received: 14 March 2023 | Revised: 20 May 2023 | Accepted: 02 June 2023

Research Article
Journal of Research and Review in Science
21-34, Volume 10, June 2023.
DOI: 10.36108/jrrslasu/3202.01.0120

ORIGINAL RESEARCH

Parcellation of Brain Magnetic Resonance Images using Improved Atlases Selection Model

Patrick Owate[1,2], Benjamin Aribisala[2,3], Charles Uwadia[1] and Philip Adewole[1]

[1]*Department of Computer Sciences, University of Lagos, Akoka*

[2]*Department of Computer Science, Lagos State University, Ojo*

[3]*Brain Research Imaging Centre, University of Edinburgh, Edinburgh, UK*

Correspondence
Patrick Owate, Department of Computer Science, Faculty of Science, Lagos State University, Nigeria.
Email:powate@yahoo.com

Funding information
Grant sponsor and grant number: NUC Research Grant (nuc.edu.ng) (NUC1311/1)

Abstract:
Introduction: Multiple atlas-based parcellation model has been demonstrated to perform better than single atlas-based parcellation model in terms of accuracy of the parcellation of human brain Magnetic Resonance Images (MRI). The weakness of the existing multiple atlas-based parcellation models is that the level of accuracy is limited if used for ageing brain due to the presence of age-related changes such as atrophy.
Aims: The aim of this study is to develop a novel multiple atlases selection model that ensures improved accuracy for the parcellation of ageing brain by combining Cost function with Similarity metric and Atrophy measure for atlases selection. This model is called COSA..
Methods:A dataset with ten brain MRI and ten atlases were used. A brain MRI was used one at a time as the target image while the remaining images constituted the source images. Using each target image, consensus atlases were obtained for COSA from the combination of cost function, similarity index and atrophy measure. These atlases were consequently used to parcellate the target image. Performance was assessed using Dice Coefficient and COSA was compared with existing atlases selection models. The existing atlases selection models investigated were Normalized Mutual Information (NMI), Mutual Information (MI), Correlation Ratio (CR), Normalized Correlation Ratio (NCR) and Least Square Error (LSE).
Results: Mean of Dice Coefficient: COSA = 0.7495196, NMI = 0.7479508, MI = 0.7473333, Jaccard Index = 0.7392522, CR = 0.7358384, NC = 0.7358043, Atrophy Measure = 0.7300867, LSE = 0.7299367, Single Atlas =0.6830223.
Conclusion: Results show that COSA performs better than the existing multiple Atlas-based models.
Keywords: Parcellation, Atlas, Human Brain, Lobar sections, Magnetic Resonance Imaging

All co-authors agreed to have their names listed as authors.

1. INTRODUCTION

Various image processing models exist for the parcellation of human brain into lobar sections**.** There are four main and distinct lobar sections, viz. Frontal lobe, Parietal lobe, Temporal lobe and Occipital lobe and each section performs different functions (Figure 1). Parcellation can be done using either manual or automated model. Manual method is the manual labeling of images by clinical expert while automated model is the usage of specific algorithms to accomplish this. Although manual model by experts is very reliable and accurate, it's tedious and time-consuming nature makes it less attractive. Therefore, automated model is preferred to manual model [1, 2]. Various image processing models have been proposed. These are supervised learning models **(**K-Nearest Neighbour Classifier, Bayesian Classifier, Algebraic techniques), unsupervised learning models **(**fuzzy C-means, K-means, and thresholding models), region growing models, shape and appearance models, energy-based models and atlas-based models. During the review of these models, atlas-based image processing model has been established to be one of the best of these models because it can divide objects of the same texture or objects with no border [3, 4, 5, 6, 7, 8, 9, 10, 11, 12, 13, 14, 15].

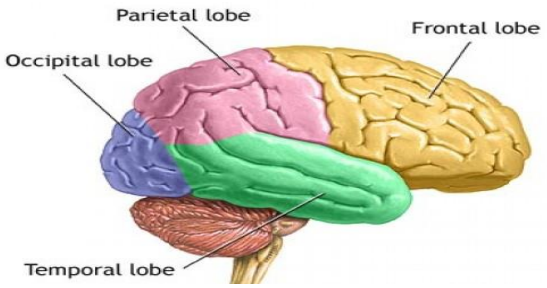

Figure 1: The Four main Lobar Sections of Human Brain

Usage of atlas-based models usually starts with either the construction of atlases or selection of existing atlases. An important stage of atlas-based model is the registration of an image (whose atlas will be used to parcellate another image) to the image that will be parcellated. Generally, the image to be parcellated is called the target image while the image used for parcellation is known as the source image. Image registration is the process of transforming an image from one coordinate into another coordinate. The registration type deployed (i.e. Linear Registration) allows adjustment of maximum of 12 parameters (i.e. rotation, translation, scaling, and shearing on *x*, *y*, and *z* coordinate axes) during transformation [16, 17, 18, 19]. In addition to the choice of image registration algorithm, it is also important to choose the type of atlas to use. There are two types of atlas selection approaches, viz. single atlas and multiple atlases. Single atlas is based on the brain of one individual while multiple atlases approach is based on brains of several subjects [20, 21]. Also, atlas type could be categorized into those that are selected from the population of subject to be parcellated and those that are selected outside the population.

The strategy applied when multiple atlases are deployed is to generate multiple parcellations of the same image using these atlases and systematically combine these parcellations in a multi-classifier framework to get a final unique parcellation [22, 23]. It has been established that even though single or multiple atlas could be used, usage of multiple atlas is more accurate than using single atlas [24, 3, 4, 20, 25, 26].

Although, various implementations of multiple atlases model have shown improvement in the accuracy of parcellation results, accuracy level could be reduced when dealing with ageing brain hence new atlases selection methods are required to solve this problem. Any human being of age 60 years and above is considered to have ageing brain [27, 28, 29, 30, 31, 32]. A top research priority is the development or identification of an image processing model with improved accuracy for the parcellation of ageing brain. In this study a novel Atlases Selection Model (ASM) is developed. The proposed model combines **Co**st function with **S**imilarity metric and **A**trophy measure for atlases selection. This atlases selection model is called **COSA** atlases selection model.

Various image processing models have been proposed for the parcellation of human brain MR images into lobar sections but most of the existing models were developed for young adults. The existing atlas-based models are single and multiple atlas-based model. The single atlas used for single atlas-based model is selected from the same data set to be parcellated or from outside the data set. The ASMs used for the existing multiple atlas parcellation models are mainly cost functions e.g. Correlation Ratio, Least Squares, Mutual Information, Normalised Correlation and Normalised Mutual Information [33, 34, 35, 36, 37]. When these methods are deployed for the parcellation of ageing brain, they have limited accuracy due to the presence of age-related problems e.g. atrophy and white matter hyperintensities [38, 39, 40]. The aim of this study is to develop a robust multiple atlases selection model that ensures improved accuracy for the parcellation of ageing brain with minimum human intervention. To accomplish this aim, the following steps will be carried out:

Step 1: The existing multiple Atlas-based models (i.e. Cost function models) will be used for atlases selection.

Step 2: Develop an atlas-based scheme that uses similarity index for atlases selection.

Step 3: Develop an atlas-based scheme that does atlases selection using atrophy measure.

Step 4: Develop an atlas-based scheme that combines cost function, similarity index and atrophy measure for atlases selection.

2. MATERIAL AND METHODS

2.1 Materials

The dataset used in this study comprises of ten high resolution anatomical (T1-weighted) brain Magnetic Resonance (MR) images with ten accompanying atlases of the images. These images were obtained from the University of Edinburgh.
This dataset is a subset of the 700 members of the Lothian Birth Cohort 1936 (LBC1936) [41, 42, 43]. The surviving participants of the Scottish Mental Survey of 1947 living in the Lothian (Edinburgh) area of Scotland constitute the LBC1936 [44, 42]. These participants undertook some tests including detailed cognitive and medical assessment at the mean age of 70 years [41, 42].

2.1.1 Brain MRI Acquisition

Brain MR imaging was performed on a 1.5T GE Signa Horizon HDxt scanner (General Electric, Milwaukee, WI, USA) using a self-shielding gradient set with a maximum gradient strength of 33 mT/m, and an 8-channel phased-array head coil. The resolution of T1-weighted images is 1 mm isotropic.

2.1.1 Image Pre-Processing

After image acquisition, MRI whole brain images were exported in Digital Imaging and Communications in Medicine (DICOM) format and as 2D images. DICOM images were then converted to 3D images and in ANALYZE format (img/hdr) to allow full 3D image visualization and processing. The atlases, comprising of frontal lobe were generated by manual delineation of the frontal lobe which was done by an experienced Neuroradiologist. Manual segmentation was performed on T1-weighted images and the mask images of the frontal lobe generated as described elsewhere [4]. In summary, segmentation was done using Analyze Software 8.1 (Mayo Clinic, Rochester, MN) [45]. T1-weighted were transformed so that the Anterior Commissure – Posterior Commissure (AC-PC) line was horizontal at the midline in sagittal orientation, and the central fissure was vertical in both coronal and axial planes. Thresholding was then applied to remove dark grey elements such as meningeal tissue and signal noise from the image [4], which resulted in clearer

grey matter CSF boundaries. The frontal lobe was then manually delineated on coronal slices of the transformed and threshold image. The final outputs of the pre-processing were the masks images of the frontal lobes for all the subjects. The preprocessing described above was done before the current study. The data used for this study were mainly the masks images of frontal lobe and the accompanied T1-weighted images.

2.2 Methods

2.2.1 Atlases selection using the existing multiple Atlas-based models (i.e. Cost function models)

From the dataset of the ten MR images, an MR image was used one at a time as the target image while the remaining images constituted the source images. In order to identify the source images that are most structurally close to each target image, all source images are required to be aligned and it is commonly done by registering all the source images to each target, using jack-knifing model [24, 4, 46, 47]. The registration is done using FMRIB Software Library, University of Oxford, UK (FSL) tools. In jack-knifing model, one image in a dataset is used one at a time as the target image and the remaining images in the dataset are used as the source images and all the source images are aligned by registering them to the selected target image. A cost function is then used to compute the closeness metrics (CM) between the selected target image and all the source images. The values of the CM are used to assign ranks to the source images. If m is the number of atlases to be selected for each target image, then the m source images with the highest CM along with their atlases are the multiple atlases for the selected target image [24, 4, 48]. The next step is to use each atlas to parcellate the target image one at a time. These parcellated images are now merged and using voting rule on the merged images, a consensus parcellated estimate for the target image is obtained [24].

Experiments were carried out using the existing multiple Atlas-based models (i.e. Cost Functions) and Figures 2 to 5 represent samples of input and output of the experiments. Figure 2 is a sample of high-resolution MR image (a) and the corresponding atlas of the Frontal Lobe of the image (b). Single atlas parcellation is illustrated using Figures 3 and 4 while multiple atlas parcellation is illustrated using Figure 5.

(a) (b)

Figure 2: Sample High Resolution MR Image (a) and the corresponding Atlas of the Frontal Lobe (b)

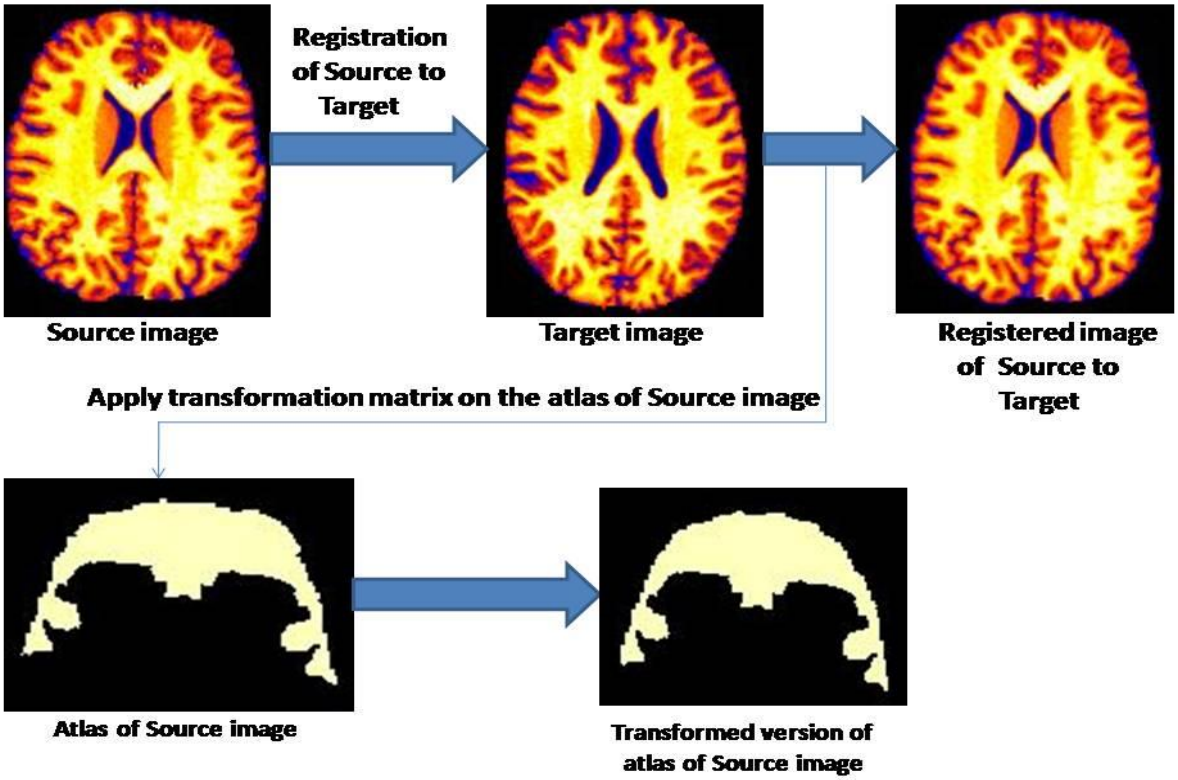

Figure 3: Registration of Source Image to Target Image and the Application of the Transformation Matrix on the Atlas of Source Image.

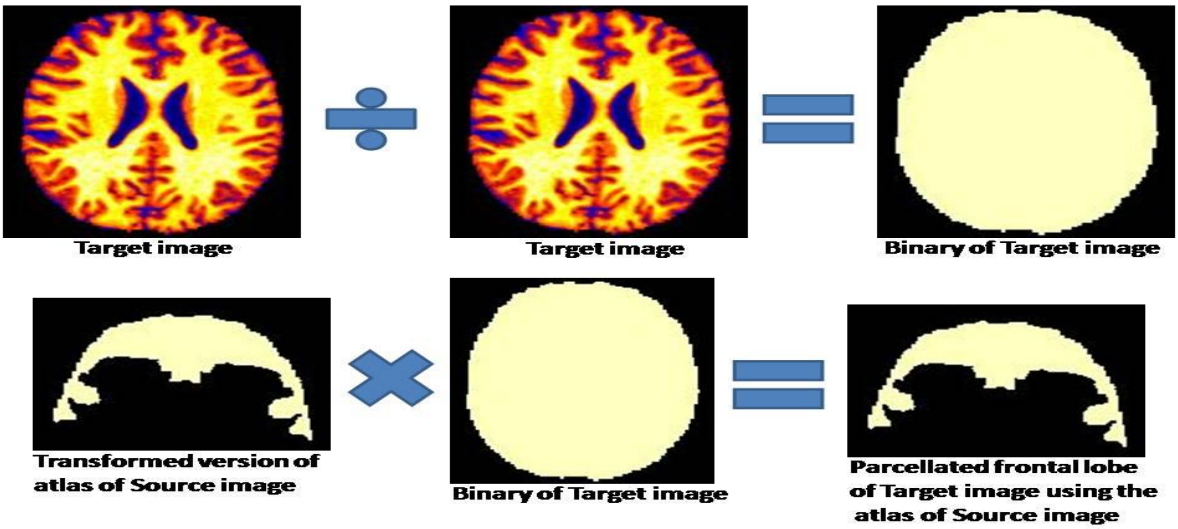

Figure 4: Parcellation of Frontal Lobe of Target Image using the Atlas of Source Image.

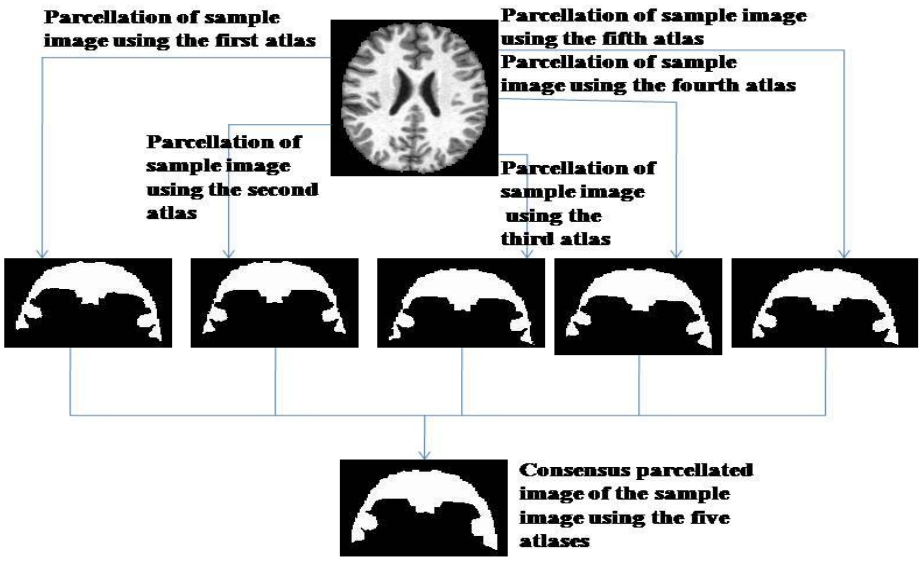

Figure 5: Multiple Atlas Parcellation of a Sample image using its five selected atlases.

2.2.2 Atlases Selection using Jaccard Index

Jaccard Index (JI) is the measure of similarity between two entities or sample sets. JI has been reported to be good as a measure of similarity of sample sets [49, 50, 51, 52, 53]. No work exists in literature to the best of the authors' knowledge that carried out atlases' selection usingJI. To construct this model, COSA usesJI. JI is referred to as "Intersection over Union" or "Jaccard Similarity Coefficient". It can be defined as the size of intersection divided by the size of the union of sample sets (Equation 2.1).

$$\mathrm{JI}(V,R) = \frac{|V \cap R|}{|V \cup R|} = \frac{|V \cap R|}{|V| + |R| - |V \cap R|} \quad \text{..... 2.1}$$

Where $\mathrm{JI}(V,R)$ is the Jaccard Index of datasets V and R, $0 \leq \mathrm{JI}(V,R) \leq 1$. The greater the value of $\mathrm{JI}(V,R)$ the closer is $V$to R.

Let R represents one MR image (target image) chosen one at a time from the dataset of ten MR images and Vrepresents one of the remaining nine MR images (source images). All the source images are registered to the target image for the source images to align. JI is computed between each chosen target image and each of its corresponding source images. If *m* is the number of atlases to be selected for each target image, then the *m* source images with the highest value of JI along with their atlases are the selected atlases for the chosen target image. Each of these atlases is used to parcellate the target image one at a time. The next step is to merge these parcellated images and use voting rule on the merged image to obtain the consensus parcellated images [24].

2.2.3 Atlases Selection using Atrophy Measure

Atrophy describes a loss of brain tissue, and it is more prevalent in ageing brain [28, 30, 31]. To the best of authors' knowledge, there is no work in literature where usage of atrophy for atlases selection has been proposed. Atrophy can be calculated by computing the volume of a particular tissue and then dividing by the Intra Cranial Volume (ICV) (Equation 2.2 and 2.3) [54]. To compute brain atrophy, COSA deploys the brain tissue segmentation technique as implemented in FSL to segment each of the images into the three

tissue classes, viz. Grey Matter (GM), White Matter (WM) and Cerebrospinal Fluid (CSF). COSA computes the volumes of these tissue classes for each image in both source images and target images datasets. Total Brain Volume (*TBV*) and Intra Cranial Volume of the images are also computed. Total Brain Volume is the sum of the volume of Grey Matter and White Matter (Equation 2.4), while Intra Cranial Volume is the sum of the volume of Grey Matter, White Matter and Cerebrospinal Fluid (Equation 2.5).

Atrophy for Grey and White Matters are computed as follows:

$AG = \frac{GM}{ICV}$ 2.2

Where AG is the Atrophy for Grey Matter.

$AW = \frac{WM}{ICV}$..... 2.3

Where AW is the Atrophy for White Matter.

The Total Brain Volume and Intra Cranial Volume are computed as follows:

$TBV = GM + WM$ 2.4

Where TBV is the Total Brain Volume, GM is the volume of Grey Matter and WM is the volume of White Matter.

$ICV = GM + WM + CSF$ 2.5

Where ICV is Intra Cranial Volume and CSF is the volume of Cerebrospinal Fluid.

To select *m* source images that are the atlases of each target image, the sum of AG and AW are computed for all images in both source and target images datasets. The *m* source images whose sum of AG and AW are closest to the sum of AG and AW of a target image along with their atlases are the selected atlases for such target image. Each of these atlases is used to parcellate the target image one at a time. The parcellated images are merged and a consensus parcellated image is obtained using voting rule on the merged image [24].

2.2.3 Atlases Selection using Combination of Cost Function, JI and Atrophy Measure

This method of atlases selection uses the combination of cost function, JI and atrophy measure to select atlases. This method is proposed in order to improve the accuracy of brain MRI parcellation of ageing brains. To the best knowledge of the authors, no work in literature has used this combination for atlases selection. In order to accomplish this method of atlases selection, COSA identifies the cost function with the highest value of CM between its consensus parcellated image and the atlas of the target image. This is the cost function whose consensus parcellated image is structurally closest to the atlas of the target image. The atlases used to construct the consensus parcellated image of the cost function with the highest CM are combined with those used for the construction of the consensus parcellated images for JI and Atrophy Measure. From this new set of datasets, the atlases of COSA will be selected for the target image. If *m* is the number of atlases to be selected for each target image using COSA, then the *m* images in the new dataset that are structurally closest to the target image along with their atlases constitute the atlases of the target image. Each of these atlases is used to parcellate the target image one at a time. The parcellated images are merged in order to obtain a consensus parcellated image using voting rule on the merged image [24].

2.2.5 Performance Evaluation of the Proposed Model

In this study Dice Coefficient (*DC*) was used to assess performance and to compare the level of performance of the ASMs investigated with that of the proposed model. DC is a measure of similarity between two sets. Other methods e.g. NCR, MI, and JI can also be used to compute similarities between two sets [55, 56, 57]. The choice of *DC* as evaluation metric is because *DC* is the most used metric in validating medical volume segmentation [57]. Although NCR, MI, and JI can be used to compute similarities between two sets, they were used for atlases selection, but *DC* was not used for atlases selection. In addition, *DC* is better than JI because *DC* can properly handle sets with real-value or weighted sets or any pair of vectors but JI cannot [58]. The *DC* between two images *A* and *B* is denoted by $DC(A,B)$ and is represented by equation 3.1.

$DC(A,B) = \frac{2|A \cap B|}{|A|+|B|}$ 3.1

where |*A*| and |*B*| are the cardinalities of the two images (i.e. the number of pixels in each image). Dice Coefficient between two images is equal to twice the number of pixels common to both images divided by the sum of the number of pixels in each image [55, 57]. The values of *DC* range from 0 to 1. The higher the value of *DC* between two images, the closer the two images. The performance of an atlas selection model *X* is better than model *Y*, if the value of *DC* between the consensus parcellated image obtained from model *X* and the corresponding atlas is higher than the value of *DC* between the consensus parcellated image obtained from model *Y* and the corresponding atlas.

In measuring the level of accuracy of ASMs, the performance level metric (equation 3.1) is used. The experiments focused on the parcellation of frontal lobe using brain MRI. Table 1 shows the performance level of various ASMs on ten brain MRI using DC as the evaluation metric.

Table 1: Performance Level of various ASMs on ten Brain MRIs using DC as the evaluation metric

Images	Single Atlas	Multiple atlases using cost functions					Jaccard Index (JI)	Atrophy Measure	Combination of Normal-ised Mutual Information, JI and Atrophy (COSA)
		Correlation Ratio`	Least Squares	Mutual Information	Normalised Correlation	Normalised Mutual Information			
1	0.6729558	0.7382275	0.7382275	0.7581789	0.7382275	0.7643540	0.7382275	0.7356983	0.7727461
2	0.6754995	0.7555645	0.7397767	0.7555645	0.7555645	0.7555645	0.7555645	0.7439875	0.7070047
3	0.7030021	0.7610265	0.7223458	0.7610265	0.7223458	0.7610265	0.7610265	0.7574418	0.7696763
4	0.7054791	0.7312509	0.7312509	0.7312509	0.7312509	0.7312509	0.7229624	0.7222743	0.7181073
5	0.6865243	0.7010146	0.7010146	0.7284227	0.7229988	0.7284227	0.7284227	0.7168340	0.7356469
6	0.6893876	0.7381702	0.7160653	0.7531888	0.7381702	0.7531888	0.7531888	0.7391046	0.7540020
7	0.6737958	0.7720316	0.7720316	0.7887973	0.7720316	0.7887973	0.7720316	0.7271628	0.7779799
8	0.6817985	0.7010837	0.7186404	0.7010837	0.7186404	0.7010837	0.7010837	0.7038057	0.7328400
9	0.6735721	0.7307211	0.7307211	0.7491171	0.7307211	0.7491171	0.7307211	0.7260024	0.7490728
10	0.6682078	0.7292933	0.7292933	0.7467024	0.7280920	0.7467024	0.7292933	0.7285557	0.7781199
Mean	0.6830223	0.7358384	0.7299367	0.7473333	0.7358043	0.7479508	0.7392522	0.7300867	0.7495196

3. RESULTS AND DISCUSSION

3.1 Atlases Selection using Jaccard Index (JI)

JI was compared with Cost Functions and Single atlas for atlases selection and the result obtained is highlighted in Figure 6. In Table 1, the average DC for the dataset using JI for atlases selection is 0.7392522. This performance is better than that of CR (DC = 0.7358384), NCR (DC = 0.7358043), LSE (DC = 0.7299367) and Single atlas (DC = 0.6830223). The average DC when JI is used for selection is less than those of NMI (DC = 0.7479508) and MI (DC = 0.7473333) because when standing alone, atlases selection using JI may not yield the best result.

3.2 Atlases Selection using Atrophy Measure

Atrophy Measure was compared with Cost Functions and Single atlas for atlases selection and the result obtained is shown in Figure 7. In Table 1, Atrophy measure for atlases selection performs better than LSE (DC = 0.7299367) and Single atlas (DC = 0.6830223). However, the performance of Atrophy measure (DC = 0.7300867) is not as good as those of NMI (DC = 0.7479508), MI (DC = 0.7473333), CR (DC = 0.7358384) and NCR (DC = 0.7358043). This is due to the fact that when used alone for atlases selection Atrophy measure may not produce the best result, even though it accounts for atrophy in ageing brain.

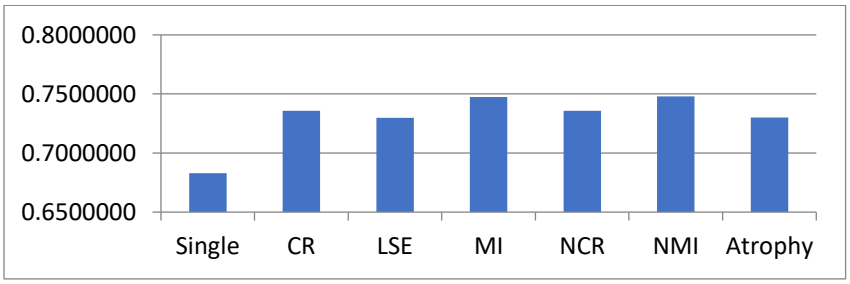

Figure 7: Average DC using Cost Functions, Single Atlas and Atrophy Measure for Atlases Selection

3.2 Combination of Normalised Mutual Information (NMI), JI and Atrophy Measure for Atlases Selection (COSA)

Combination of NMI, JI and Atrophy Measure was compared with Cost Functions and Single atlas for atlases selection and the result obtained is highlighted in Figure 8. In Table 1, the average DC for the dataset when COSA model is used for atlases selection is 0.7495196. This performance is the best when compared with NMI (DC = 0.7479508), MI (DC = 0.7473333), CR (DC = 0.7358384), NCR (DC = 0.7358043), LSE (DC = 0.7299367) and Single atlas (DC = 0.6830223).

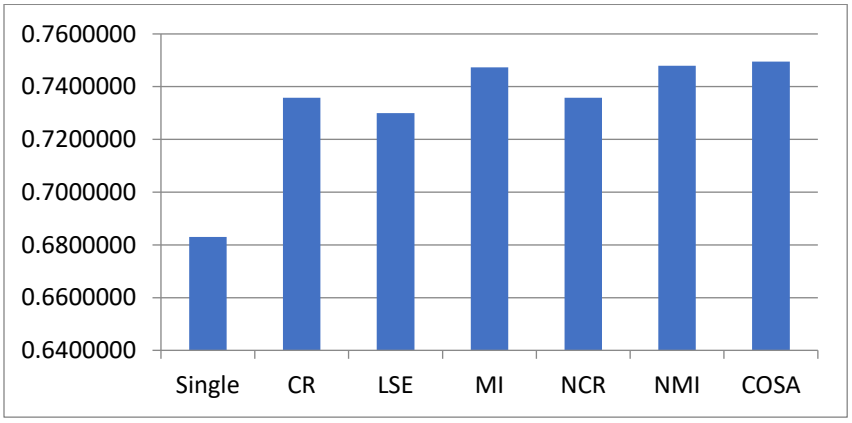

Figure 8: Average DC using Cost Functions, Single Atlas and COSA model for Atlases Selection

4. CONCLUSION

The aim of this study was to develop a novel atlases selection method for improved parcellation of brain MRI. The model developed is called Cost function with Similarity metric and Atrophy measure (COSA). COSA was implemented on parcellation of frontal lobe using brain MRI. Performance was measured using DC and the performance of COSA was compared with the existing multiple Atlas-based models (i.e. Cost function models) and Single atlas model.

A summary of results obtained show that COSA performed better than the existing multiple Atlas-based models and Single atlas model. The DC of COSA is greater than the DC of each of the existing multiple

Atlas-based models and Single atlas model. This shows that the degree of overlap of COSA is better than each of the existing multiple Atlas-based models and Single atlas model. Our model (i.e. COSA) is better than the existing multiple Atlas-based models and Single atlas model due to introduction of new methods of atlases selection. These methods are the usage of atrophy measure and JI for the selection of atlases.

Atlas based parcellation model have been previously reported [4] to underperform on ageing brain because of age related changes like atrophy. Our method performs better because it considers age related problem during atlases selection. This is intuitive because a method that does not consider age related changes would not normally correct for such changes during processing.

Our results were compared with the methods proposed by [59], [60], and [61] in the segmentation of the hippocampus of some Internet Brain Segmentation Repository (IBSR) datasets. The DCs were [59] = 0.59, [60] = 0.74, and [61] = 0.70. We also compared our results with these three proposed methods in the segmentation of caudate nucleus of the IBSR datasets. The DCs were [59] = 0.0.65, [60] = 0.74, and [61] = 0.76. Virtually all the results indicated that COSA performs better than all the proposed methods. However, the DC of [61] during the segmentation of caudate nucleus was higher than that of COSA. This difference may be attributed to some factors: our datasets are different from those used for their experiments (IBSR), the segmentation carried out using the three methods were done on sub-cortical structures (i.e. hippocampus and caudate nucleus) whereas our model carried out parcellation of a lobar section of the brain (i.e. frontal lobe). The sub-cortical structures have clear borders while the lobar sections do not have clear borders. Our model is atlas-based model and it has an advantage over the three methods: it is able to divide objects of the same texture or objects with no border [3, 4, 5, 6, 7, 8, 9, 10, 11, 12, 13, 14, 15].

The strengths of our proposed models are derived from some factors. These factors include the availability of ground truth, introduction of atrophy measure and objective selection of atlases.
Assessment of percellation algorithm is normally limited by the lack of ground truth. This is because ground truths are always difficult to get because an expert is required to generate them. In our study, we had access to the ground truth. We used the ground truth generated by a Neuroradiologist. This suggests that our results can be trusted.

The second strength is the introduction of atrophy-based selection. Ageing brain is normally affected by age related changes such as atrophy and the presence of white matter hyperintensities [4]. The existing atlas-based models do not consider those changes as we did in our study. This approach makes the proposed method unique and our result shows that the proposed method is very promising because it performed better than those methods that do not consider atrophy during percellation.

The third strength of this study is the objective selection of atlases. Existing methods always use one or a set of representative atlases. Representative atlases are not good because atrophy can occur in any part of the brain thereby making it difficult to identify a single brain (or a set of brains) that will be truly representative. We used multiple atlases. Each set of atlases was empirically selected by performing many experiments to ensure that the age-related brain changes are well captured. This suggests that our method is not only reproducible, but can also be trusted.

The study has some limitations. One, we used linear registration for aligning the images. Linear registration is known to underperform in comparison with non-linear registration because linear registration is restricted to a maximum of 12 affine transformation [62, 17, 18, 19]. We could not use Non-linear registration because of lack of computational resources (i.e. server of high processing power). However, our target was to build a model that will improve percallation by considering atrophy selection. The aim of the study was achieved because the proposed algorithm performed better than the existing models. We are convinced that the use of non linear registration will further improve our model and that is noted for future research. The second limitation is the sample size. We used only ten anatomical MR images along with their corresponding atlases. This was due to the fact that we do not have access to more images. We would have manually segmented more images and obtain their ground truths, but we do not have the expertise to do so at the current time. Even if we decide to make use of the services of radiologist, we do not have the appropriate images that could be used to carry out such exercise. Future work should consider using more images. The

third limitation of the study is the use of foreign images. We could not use local images (images acquired in Nigeria) because of lack of funds. There are very few 1.5 Tesla (1.5T) MRI scanners in Nigeria and the cost of acquisition of images from these scanners is enormous. Future research should consider acquiring images in Nigeria.

In conclusion, Atlas-based models that use combination of atrophy measure, JI and cost functions perform better than the existing multiple Atlas-based models (i.e. Cost function models) and Single atlas model.

ACKNOWLEDGEMENTS

The authors would love to thank Professor Rahman M.A., Mr. Bamiro A.B., and Mr. Adeyemi M.A. of Department of Computer Science, Lagos State University for their help during laboratory experiments, most especially the installation of tools used for the experiments. We also appreciate Mrs. Omotoso R.A. and Mrs. Omoniyi O.B. of the same department for all the help in the area of administrative tasks.

AUTHORS' CONTRIBUTIONS

All authors read and approved the final manuscript.

REFERENCES

[1] Hosseini, M.-P., Nazem-Zadeh, M.-R., Pompili, D., Jafari-Khouzani, K., Elisevich, K., and Soltanian-Zadeh, H. (2016). Automatic and manual segmentation of hippocampus in epileptic patients mri. arXiv preprint arXiv:1610.07557.
[2] Moghaddam, M. J., and Soltanian-Zadeh, H. (2009). Automatic segmentation of brain structures using geometric moment invariants and artificial neural networks. Inf Process Med Imaging 21, 326-37.
[3] Alruwaili, A. R., Pannek, K., Henderson, R. D., Gray, M., Kurniawan, N. D., and McCombe, P. A. (2020). Serial MRI studies over 12 months using manual and atlas-based region of interest in patients with amyotrophic lateral sclerosis. BMC medical imaging 20, 1-10.
[4] Aribisala, B. S., Cox, S. R., Ferguson, K. J., MacPherson, S. E., MacLullich, A. M., Royle, N. A., Hernández, M. V., Bastin, M. E., Deary, I. J., and Wardlaw, J. M. (2013). Assessing the performance of atlas-based prefrontal brain parcellation in an ageing cohort. Journal of computer assisted tomography 37.
[5] Babalola, K. O., Cootes, T. F., Twining, C. J., Petrovic, V., and Taylor, C. (2008). 3D brain segmentation using active appearance models and local regressors. In "International Conference on Medical Image Computing and Computer-Assisted Intervention", pp. 401-408. Springer.
[6] Babalola, K. O., Patenaude, B., Aljabar, P., Schnabel, J., Kennedy, D., Crum, W., Smith, S., Cootes, T., Jenkinson, M., and Rueckert, D. (2009). An evaluation of four automatic methods of segmenting the subcortical structures in the brain. Neuroimage 47, 1435-1447.
[7] González-Vill, S., and Valverde, A. O. S. (2016). A review on brain structures segmentation in magnetic. Lancet Neurology 15, 292-303.
[8] Igual, L., Soliva, J. C., Hernández-Vela, A., Escalera, S., Jiménez, X., Vilarroya, O., and Radeva, P. (2011). A fully-automatic caudate nucleus segmentation of brain MRI: application in volumetric analysis of pediatric attention-deficit/hyperactivity disorder. Biomedical engineering online 10, 105.
[9] Liu, Y., Zhao, G., Nacewicz, B. M., Adluru, N., Kirk, G. R., Ferrazzano, P. A., Styner, M., and Alexander, A. L. (2019). Accurate Automatic Segmentation of Amygdala Subnuclei and Modeling of Uncertainty via Bayesian Fully Convolutional Neural Network. arXiv preprint arXiv:1902.07289.
[10] Owate, P., Aribisala, B., Uwadia, C., and Adewole, P. (2017). Systematic Review of Computational Models for Human Brain Parcellation. Journal of Research and Review in Science.
[11] Peer, M., Nitzan, M., Bick, A. S., Levin, N., and Arzy, S. (2017). Evidence for functional networks within the human brain's white matter. Journal of Neuroscience 37, 6394-6407.
[12] Sakamoto, M., Hiasa, Y., Otake, Y., Takao, M., Suzuki, Y., Sugano, N., and Sato, Y. (2019). Automated Segmentation of Hip and Thigh Muscles in Metal Artifact-Contaminated CT using Convolutional Neural Network-Enhanced Normalized Metal Artifact Reduction. arXiv preprint arXiv:1906.11484.
[13] Van Ginneken, B., Heimann, T., and Styner, M. (2007). 3D segmentation in the clinic: A grand challenge. 3D segmentation in the clinic: a grand challenge, 7-15.

[14] Wu, Y., Jiang, J.-H., Chen, L., Lu, J.-Y., Ge, J.-J., Liu, F.-T., Yu, J.-T., Lin, W., Zuo, C.-T., and Wang, J. (2019). Use of radiomic features and support vector machine to distinguish Parkinson's disease cases from normal controls. Annals of Translational Medicine 7.
[15] Zbontar, J., Knoll, F., Sriram, A., Muckley, M. J., Bruno, M., Defazio, A., Parente, M., Geras, K. J., Katsnelson, J., and Chandarana, H. (2018). fastMRI: An open dataset and benchmarks for accelerated MRI. arXiv preprint arXiv:1811.08839.
[16] Lima, A. A., Mridha, M. F., Das, S. C., Kabir, M. M., Islam, M. R., and Watanobe, Y. (2022b). A Comprehensive Survey on the Detection, Classification, and Challenges of Neurological Disorders. Biology 11, 469.
[17] Wang, Z., Huo, X., Chen, Z., Zhang, J., Sheng, L., and Xu, D. (2022). Improving RGB-D Point Cloud Registration by Learning Multi-scale Local Linear Transformation. arXiv preprint arXiv:2208.14893.
[18] Yagis, E. (2022). Diagnosis of Neurodegenerative Diseases using Deep Learning, University of Essex.
[19] Zhang, X., Feng, Y., Chen, W., Li, X., Faria, A. V., Feng, Q., and Mori, S. (2019). Linear registration of brain mri using knowledge-based multiple intermediator libraries. Frontiers in neuroscience 13, 909.
[20] Heckemann, R. A., Keihaninejad, S., Aljabar, P., Rueckert, D., Hajnal, J. V., Hammers, A., and Initiative, A. s. D. N. (2010). Improving intersubject image registration using tissue-class information benefits robustness and accuracy of multi-atlas based anatomical segmentation. Neuroimage 51, 221-227.
[21] Holmberg, M., Malmgren, H., Heckemann, R. A., Johansson, B., Klasson, N., Olsson, E., Skau, S., Starck, G., and FilipssonNyström, H. (2022). A Longitudinal Study of Medial Temporal Lobe Volumes in Graves Disease. The Journal of Clinical Endocrinology & Metabolism 107, 1040-1052.
[22] Han, X., Hoogeman, M. S., Levendag, P. C., Hibbard, L. S., Teguh, D. N., Voet, P., Cowen, A. C., and Wolf, T. K. (2008). Atlas-based auto-segmentation of head and neck CT images. In "International Conference on Medical Image Computing and Computer-Assisted Intervention", pp. 434-441. Springer.
[23] Rohlfing, T., and Maurer Jr, C. R. (2005). Multi-classifier framework for atlas-based image segmentation. Pattern Recognition Letters 26, 2070-2079.
[24] Aljabar, P., Heckemann, R. A., Hammers, A., Hajnal, J. V., and Rueckert, D. (2009). Multi-atlas based segmentation of brain images: atlas selection and its effect on accuracy. Neuroimage 46, 726-738.
[25] Rohlfing, T., Zahr, N. M., Sullivan, E. V., and Pfefferbaum, A. (2010). The SRI24 multichannel atlas of normal adult human brain structure. Hum Brain Mapp 31, 798-819.
[26] Zhao, J., Ge, H., He, W., Li, Y., Shi, W., Jiang, Z., Li, Y., and Li, X. (2021). A Segmentation Method of Foramen Ovale Based on Multiatlas. Computational and Mathematical Methods in Medicine 2021.
[27] Bischof, A., Papinutto, N., Keshavan, A., Rajesh, A., Kirkish, G., Zhang, X., Mallott, J. M., Asteggiano, C., Sacco, S., and Gundel, T. J. (2022). Spinal cord atrophy predicts progressive disease in relapsing multiple sclerosis. Annals of Neurology 91, 268-281.
[28] Eshaghi, A., Prados, F., Brownlee, W. J., Altmann, D. R., Tur, C., Cardoso, M. J., De Angelis, F., Van De Pavert, S. H., Cawley, N., and De Stefano, N. (2018). Deep gray matter volume loss drives disability worsening in multiple sclerosis. Annals of neurology 83, 210-222.
[29] Evans, M. C., Barnes, J., Nielsen, C., Kim, L. G., Clegg, S. L., Blair, M., Leung, K. K., Douiri, A., Boyes, R. G., and Ourselin, S. (2010). Volume changes in Alzheimer's disease and mild cognitive impairment: cognitive associations. European radiology 20, 674-682.
[30] Gu, T., Fu, C., Shen, Z., Guo, H., Chen, M., Rockwood, K., and Song, X. (2019). Age-related whole-brain structural changes in relation to cardiovascular risks across the adult age spectrum. Frontiers in aging neuroscience 11, 85.
[31] Hedman, A. M., van Haren, N. E., Schnack, H. G., Kahn, R. S., and Hulshoff Pol, H. E. (2012). Human brain changes across the life span: a review of 56 longitudinal magnetic resonance imaging studies. Human brain mapping 33, 1987-2002.
[32] Sastre-Garriga, J., Pareto, D., Battaglini, M., Rocca, M. A., Ciccarelli, O., Enzinger, C., Wuerfel, J., Sormani, M. P., Barkhof, F., and Yousry, T. A. (2020). MAGNIMS consensus recommendations on the use of brain and spinal cord atrophy measures in clinical practice. Nature Reviews Neurology 16, 171-182.
[33] Dong, H.-M., Castellanos, F. X., Yang, N., Zhang, Z., Zhou, Q., He, Y., Zhang, L., Xu, T., Holmes, A. J., and Yeo, B. T. (2020). Charting brain growth in tandem with brain templates at school age. Science Bulletin 65, 1924-1934.
[34] Klein, A., Ghosh, S. S., Bao, F. S., Giard, J., Häme, Y., Stavsky, E., Lee, N., Rossa, B., Reuter, M., and Neto, E. C. (2017). Mindboggling morphometry of human brains. PLoS computational biology 13.
[35] Klein, A., Mensh, B., Ghosh, S., Tourville, J., and Hirsch, J. (2005). Mindboggle: automated brain labeling with multiple atlases. BMC medical imaging 5, 7.

[36] Sanroma, G., Wu, G., Gao, Y., and Shen, D. (2014). Learning to rank atlases for multiple-atlas segmentation. IEEE transactions on medical imaging 33, 1939-1953.
[37] Tran, P. V. (2016). A fully convolutional neural network for cardiac segmentation in short-axis MRI. arXiv preprint arXiv:1604.00494.
[38] Cabezas, M., Oliver, A., Llado, X., Freixenet, J., and Cuadra, M. B. (2011). A review of atlas-based segmentation for magnetic resonance brain images. Computer methods and programs in biomedicine 104, e158-77.
[39] Lundervold, A. S., and Lundervold, A. (2019). An overview of deep learning in medical imaging focusing on MRI. ZeitschriftfürMedizinischePhysik 29, 102-127.
[40] Renard, F., Guedria, S., De Palma, N., and Vuillerme, N. (2020). Variability and reproducibility in deep learning for medical image segmentation. Scientific Reports 10, 1-16.
[41] Deary, I. J., Gow, A. J., Pattie, A., and Starr, J. M. (2012). Cohort profile: the Lothian Birth Cohorts of 1921 and 1936. International journal of epidemiology 41, 1576-1584.
[42] Deary, I. J., Gow, A. J., Taylor, M. D., Corley, J., Brett, C., Wilson, V., Campbell, H., Whalley, L. J., Visscher, P. M., and Porteous, D. J. (2007). The Lothian Birth Cohort 1936: a study to examine influences on cognitive ageing from age 11 to age 70 and beyond. BMC geriatrics 7, 1-12.
[43] Wardlaw, J. M., Bastin, M. E., Valdés Hernández, M. C., Maniega, S. M., Royle, N. A., Morris, Z., Clayden, J. D., Sandeman, E.
[44] Committee, S. C. f. R. i. E. M. S. (1949). "The trend of Scottish intelligence: A comparison of the 1947 and 1932 surveys of the intelligence of eleven-year-old pupils," University of London Press.
[45] Mayo, C. (2008). Analyze 8.1. AnalyzeDirect, Inc. Mayo Clinic. http://www. analyzedirect. com/Analyze/upgrade. asp.
[46] Stowell, D., Wood, M. D., Pamuła, H., Stylianou, Y., and Glotin, H. (2019). Automatic acoustic detection of birds through deep learning: the first Bird Audio Detection challenge. Methods in Ecology and Evolution 10, 368-380.
[47] Tibshirani, R. J., and Efron, B. (1993). An introduction to the bootstrap. Monographs on statistics and applied probability 57, 1-436.
[48] Raudaschl, P. F., Zaffino, P., Sharp, G. C., Spadea, M. F., Chen, A., Dawant, B. M., Albrecht, T., Gass, T., Langguth, C., and Lüthi, M. (2017). Evaluation of segmentation methods on head and neck CT: auto-segmentation challenge 2015. Medical physics 44, 2020-2036.
[49] Berman, M., and Blaschko, M. B. (2017). Optimization of the jaccard index for image segmentation with the lovász hinge. CoRR, abs/1705.08790 5.
[50] Fletcher, S., and Islam, M. Z. (2018). Comparing sets of patterns with the Jaccard index. Australasian Journal of Information Systems 22.
[51] LopatkoLindman, K., Jonsson, C., Weidung, B., Olsson, J., Pandey, J. P., Prokopenko, D., Tanzi, R. E., Hallmans, G., Eriksson, S., and Elgh, F. (2022). PILRA polymorphism modifies the effect of APOE4 and GM17 on Alzheimer's disease risk. Scientific Reports 12, 1-8.
[52] Prokopenko, D., Hecker, J., Silverman, E. K., Pagano, M., Nöthen, M. M., Dina, C., Lange, C., and Fier, H. L. (2016). Utilizing the Jaccard index to reveal population stratification in sequencing data: a simulation study and an application to the 1000 Genomes Project. Bioinformatics 32, 1366-1372.
[53] Prokopenko, D., Lee, S., Hecker, J., Mullin, K., Morgan, S., Katsumata, Y., Weiner, M. W., Fardo, D. W., Laird, N., and Bertram, L. (2022). Region-based analysis of rare genomic variants in whole-genome sequencing datasets reveal two novel Alzheimer's disease-associated genes: DTNB and DLG2. Molecular psychiatry 27, 1963-1969.
[54] Aribisala, B. S., Akinyemi, R. O., Ogbole, G. I., Firbank, M., Rahman, M. A., Enikuomehin, O. A., Akinyemi, J. O., Owate, P., Adebayo, P. B., Aiyeniko, O., Owolabi, M. O., Allan, L., Ogunseyinde, O., Kalaria, R. N., and AOgunniyi, A. (2017). Brain atrophy in African stroke survivors: The CogFAST Nigeria study. Afr. J. Med. Med. Sci. 46.
[55] Myers, P. E., Arvapalli, G. C., Ramachandran, S. C., Pisner, D. A., Frank, P. F., Lemmer, A. D., Bridgeford, E. W., Nikolaidis, A., and Vogelstein, J. T. (2019). Standardizing human brain parcellations. BioRxiv, 845065.
[56] Taha, A. A., and Hanbury, A. (2015). Metrics for evaluating 3D medical image segmentation: analysis, selection, and tool. BMC medical imaging 15, 1-28.
[57] Yaegashi, Y., Tateoka, K., Fujimoto, K., Nakazawa, T., Nakata, A., Saito, Y., Abe, T., Yano, M., and Sakata, K. (2012). Assessment of similarity measures for accurate deformable image registration. J. Nucl. Med. Radiat. Ther 42, 12.

[58] Binanto, I., Warnars, H. L. H. S., Abbas, B. S., Heryadi, Y., Sianipar, N. F., and Sanchez, H. E. P. (2018). Comparison of similarity coefficients on morphological rodent tuber. In "2018 Indonesian Association for Pattern Recognition International Conference (INAPR)", pp. 104-107. IEEE.
[59] Tsai, A., Wells, W., Tempany, C., Grimson, E., and Willsky, A. (2004). Mutual information in coupled multi-shape model for medical image segmentation. Medical Image Analysis 8, 429-445.
[60] Akhoundi-Asl, A., and Soltanian-Zadeh, H. (2007). Nonparametric entropy-based coupled multi-shape medical image segmentation. In "Biomedical Imaging: From Nano to Macro, 2007. ISBI 2007. 4th IEEE International Symposium on", pp. 1200-1203. IEEE
[61] Asl, A. A., and Soltanian-Zadeh, H. (2008). Constrained optimization of nonparametric entropy-based segmentation of brain structures. In "2008 5th IEEE International Symposium on Biomedical Imaging: From Nano to Macro", pp. 41-44. IEEE.
[62] Lima, A., Mridha, M., Sujoy, C., Kabir, M., Islam, M., and Watanobe, Y. (2022a). A Comprehensive Survey on the Detection, Classification, and Challenges of Neurological Disorders. Biology 2022, 11, 469. s Note: MDPI stays neutral with regard to
jurisdictional claims in published